Study of 5-azidomethyl-8-hydroxyquinoline structure by X-ray diffraction and HF-DFT computational methods

H. Bougharraf, R. Benallal, T. Sahdane, D. Mondieig, Ph. Negrier, S. Massip, M. Elfaydy, B. Lakhrissi, B. Kabouchi

Study of 5-Azidomethyl-8-hydroxyquinoline Structure by X-ray Diffraction and HF–DFT Computational Methods[1]

H. Bougharraf[a,*], R. Benallal[a], T. Sahdane[a], D. Mondieig[b], Ph. Negrier[b], S. Massip[c], M. Elfaydy[d], B. Lakhrissi[d], and B. Kabouchi[a]

[a] *Equipe de Spectronomie Moléculaire, Optique et Instrumentation Laser, Université Mohammed V, Faculté des Sciences, B. P 1014, Rabat, Morocco*

[b] *Laboratoire Ondes et Matière d'Aquitaine, Université de Bordeaux, 33405 Talence, France*

[c] *Institut Européen de Chimie et Biologie, 33607 Pessac, France*

[d] *Laboratoire d'Agroressources Polymères et Génie des Procédés, Université Ibn Tofail, Faculté des Sciences, B.P 133, Kénitra, Morocco*

**e-mail: hafida.bougharraf@gmail.com*

Abstract—5-Azidomethyl-8-hydroxyquinoline has been synthesized and characterized using IR, ^{1}H and ^{13}C NMR spectroscopic methods. Thermal analysis revealed no solid-solid phase transitions. The crystal structure of this compound was refined by Rietveld method from powder X-ray diffraction data at 295 K. The single-crystal structure of the compound at 260 K was solved and refined using SHELX 97 program. According to the data obtained by both methods, the structure of the compound is monoclinic, space group $P2_1/c$, with $Z = 4$ and $Z' = 1$. For the single crystal at 260 K, $a = 12.2879$ (9) Å, $b = 4.8782$ (3) Å, $c = 15.7423$ (12) Å, $\beta = 100.807(14)°$. Mechanisms of deformation resulting from intra- and intermolecular interactions, such as hydrogen bonding, induced slight torsions in the crystal structure. The optimized molecular geometry of 5-azidomethyl-8-hydroxyquinoline in the ground state is calculated using density functional theory (B3LYP) and Hartree-Fock (HF) methods with the 6-311G(*d*,*p*) basis set. The calculated results show good agreement with experimental values. Energy gap of the molecule was found using HOMO and LUMO calculation which reveals that charge transfer occurs within the molecule.

Keywords: 5-azidomethyl-8-hydroxyquinoline, X-ray diffraction, single crystal structure, hydrogen bonding, HF–DFT, HOMO–LUMO

DOI: 10.1134/S0036024417020078

1. INTRODUCTION

8-Hydroxyquinoline molecule is a widely studied ligand. It is frequently used due to its biological effects ascribed to complexation of specific metal ions, such as copper(II) and zinc(II) [1, 2]. This chelator properties determine its antibacterial action [3–5]. Aluminum(III) 8-hydroxyquinolinate has great application potential in the development of organic light-emitting diodes (OLEDs) and electroluminescent displays [6–10]. One of the serious problems of this technology is the failure of these devices at elevated temperatures. Also the use of 8-hydroxyquinoline in liquid-liquid extraction is limited because of its high solubility in acidic and alkaline aqueous solutions. In order to obtain the materials with improved properties for these specific applications, some 8-hydroxyquinoline derivatives have been synthesized. The antitumor and antibacterial properties of these compounds are extensively studied [11–15].

The literature presents X-ray crystal structure analysis of some derivatives of 8-hydroxyquinoline. It was shown, for example, that 8-hydroxyquinoline *N*-oxide crystallizes in the monoclinic system with space group $P2_1/c$, $Z = 4$, and presents intramolecular H-bonding [16]. Gavin et al. reported the synthesis of 8-hydroxyquinoline derivatives [17, 18] and their X-ray crystal structure analysis. 7-Bromoquinolin-8-ol structure was determined as monoclinic with space group $C2/c$, $Z = 8$. Its ring system is planar [11]. Recently, azo compounds based on 8-hydroxyquinoline derivatives attract more attention as chelating agents for a large number of metal ions [19, 20]. Series of heteroarylazo 8-hydroxyquinoline dyes were synthesized and studied in solution to determine the most stable tautomeric

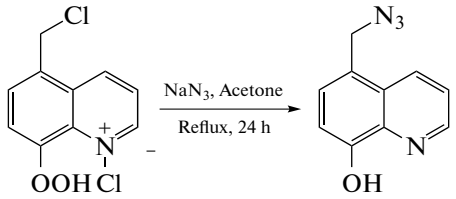

Scheme 1. Synthesis of 5-azidomethyl-8-hydroxyquinoline molecule.

form. The X-ray analysis revealed a strong intramolecular H-bond between the hydroxy H and the quinoline N atoms. This result suggests that the synthesized dyes are azo compounds stable in solid state [21].

In the present work, we choose one of the 8-hydroxyquinoline derivatives, namely 5-azidomethyl-8-hydroxyquinoline (AHQ) (Scheme 1), also known for its applicability in extraction of some metal ions. It has been inferred from literature that the structural and geometrical data of AHQ molecule have not been reported till date, although several techniques were used in order to understand its behavior in different solvents [22], but many aspects of this behavior remain unknown. Here we report for the first time the structural characterization of AHQ molecule by X-ray diffraction analysis and the results of our calculations using density functional theory (B3LYP) and Hartree-Fock (HF) methods with the 6-311G(*d*,*p*) basis set, which are chosen to study the structural, geometric and charge transfer properties of AHQ molecule in the ground state.

2. EXPERIMENTAL

2.1. Synthesis of 5-Azidomethyl-8-hydroxyquinoline

All chemicals were purchased from Aldrich or Acros (France). 5-Azidomethyl-8-hydroxyquinoline was synthesized according to the method described by Himmi et al. [22], by reaction of sodium azide with 5-chloromethyl-8-hydroxyquinoline hydrochloride in refluxing acetone for 24 h (Scheme 1).

A suspension of 5-chloromethyl-8-hydroxyquinoline hydrochloride (1 g, 4.33 mmol) in acetone (40 mL) was added dropwise to NaN_3 (1.3 g, 17 mmol) in acetone (10 mL). The mixture was refluxed for 24 h. After cooling, the solvent was evaporated under reduced pressure and the residue was partitioned between $CHCl_3/H_2O$ (150 mL, 1 : 1). The organic phase was isolated, washed with water (3 × 20 mL) and dried over anhydrous magnesium sulfate. The solvent was removed by rotary evaporation under reduced pressure to give a crude product which was purified by recrystalization from ethanol to give the pure product as white solid (0.73 g, 85%).

2.2. Characterization of 5-Azidomethyl-8-hydroxyquinoline

The structure of the product was confirmed by ^1H and ^{13}C NMR and IR spectra. Melting points were determined on an automatic IA 9200 digital melting point apparatus in capillary tubes and are uncorrected. ^1H NMR spectra were recorded on a Bruker 300 WB spectrometer at 300 MHz for solutions in DMSO-d_6. Chemical shifts are given as δ values with reference to tetramethylsilane (TMS) as internal standard. Infrared spectra were recorded from 400 to 4000 cm^{-1} on a Bruker IFS 66v Fourier transform spectrometer using KBr pellets. Mass spectrum was recorded on THERMO Electron DSQ II.

Mp: 116–118°C; IR (KBr) (cm^{-1}): ν 2090 (C–N_3, stretching); ^1H NMR (300 MHz, DMSO-d_6), δ_{ppm} = 7.04–8.90 (m, 4H, quinoline), 4.80 (s, 1H, OH), 2.48 (s, 2H, aromatic-CH_2–N_3), ^{13}C NMR (75 MHz, DMSO-d_6), δ_{ppm} = 51.38, 110.47, 122.69, 127.550, 130.03, 133.17, 139.29, 148.72, 154.54.

2.3. Differential Scanning Calorimetry

To study the thermal behavior and to verify a possible phase transition [23] for the studied product, differential scanning calorimetric (DSC) analysis using ~4 mg samples was performed on Perkin-Elmer DSC-7 apparatus. Samples were hermetically sealed into aluminum pans. The heating rate was 10 K/min.

2.4. Crystallographic Data and Structure Analysis

X-ray powder diffraction analysis was performed on an Inel CPS 120 diffractometer. The diffraction lines were collected on a 4096 channel detector over an arc of 120° and centered on the sample. The Cu$K_{\alpha 1}$ (λ = 1.5406 Å) radiation was obtained by means of a curved quartz monochromator at a voltage of 40 kV and a current of 25 mA. The powder was put in a Lindemann glass capillary 0.5 mm in diameter, which was rotated to minimize preferential orientations. The experiment providing good signal/noise ratio took approximately 8 h under normal temperature and pressure. The refinement of the structure was performed using the Materials Studio software [24]. For the monocrystal experiment, a colorless single crystal of 0.12 × 0.10 × 0.05 mm size was selected and mounted on the diffractometer Rigaku Ultrahigh instrument with microfocus X-ray rotating anode tube (45 kV, 66 mA, CuK_α radiation, λ = 1.54187 Å),

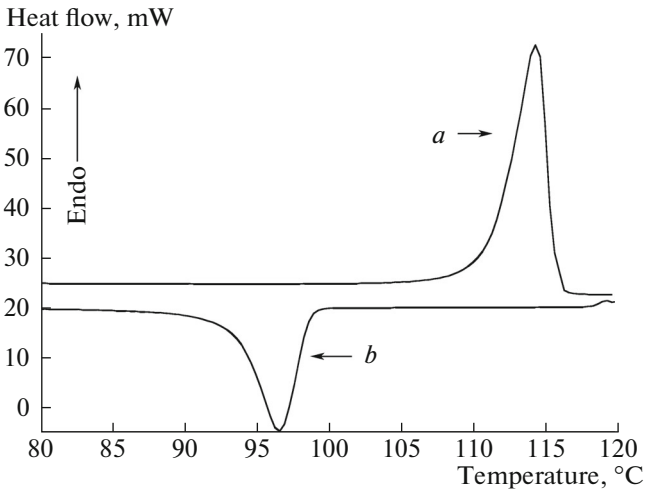

Fig. 1. DSC thermogram for AHQ material: *a*, heating and *b*, cooling.

equipped with Dectris Pilatus 200 K detector was used. The measurements were performed at 260 K. The structure was solved by direct methods using SHELXS-97 [25] program and the Crystal Clear-SM Expert 2.1 software.

2.5. Theoretical Calculations

Density functional theory (DFT) calculations were performed to determine the geometrical and structural parameters of AHQ molecule in ground state, because this approach has a greater accuracy in reproducing the experimental values in geometry. It requires less time and offers similar accuracy for middle sized and large systems. Recently it's more used to study chemical and biochemical phenomena [26, 27]. All calculations were performed with the Gaussian program package [28], using B3LYP and Hartree-Fock (HF) methods with the 6-311G(*d*,*p*) basis set. Starting geometries of compound were taken from X-ray refinement data.

3. RESULTS AND DISCUSSION

Thermal analysis revealed no solid-solid phase transitions (Fig. 1). The melting temperature (mp = 115°C) was in agreement with the value measured in capillary with visual fixation of melting point. The melting heat found by DSC for the compound was $\Delta H = 155$ J/g.

X-ray diffraction patterns for AHQ powder at 295 K (Fig. 2) show a good agreement between calculated profile and the experimental result.

The results of refinement for both powder and single crystal techniques converged practically to the same crystallographic structure. Data collection parameters are given in Table 1.

The structure of AHQ molecule and packing view calculated from single crystal diffraction data, are shown in Figs. 3 and 4, respectively.

The Fig. 3 indicates the nomination and the anisotropic displacement parameters of disordered pairs for the ORTEP drawing for AHQ molecule. Absorption corrections were carried out by the semi-empirical method from equivalent. The calculation of average values of intensities gives $R_{int} = 0.0324$ for 1622 independent reflections. A total of 6430 reflections were

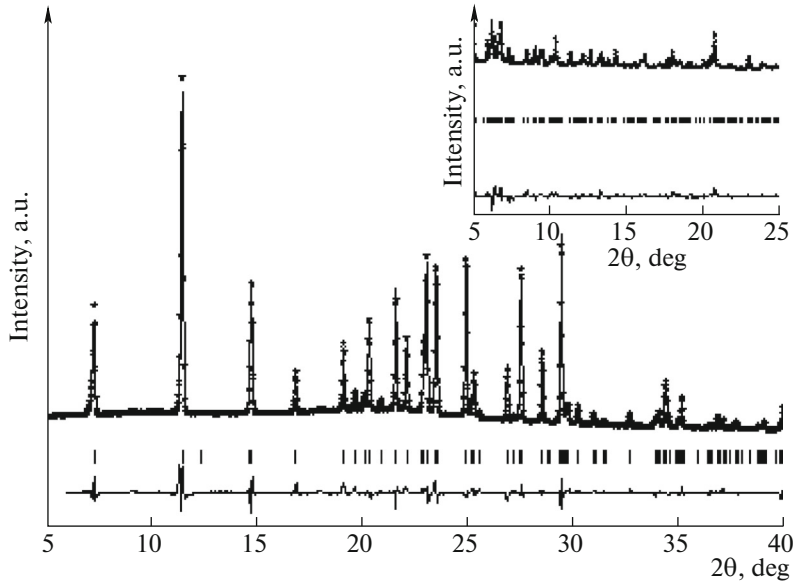

Fig. 2. Superposition of the X-ray diffraction patterns for AHQ powder at 295 K: calculated (straight line), experimental (*), Bragg reflections calculated (scatter line) and the difference between calculated and experimental (solid line).

Table 1. Crystallographic data for AHQ molecule

Parameters	Monocrystal	Powder
Temperature, K	260(2)	295
Wavelength, Å	1.54187	1.54056
Space group	$P2_1/c$	$P2_1/c$
a, Å	12.2879(9)	12.2643(12)
b, Å	4.8782(3)	4.8558(6)
c, Å	15.7423(12)	15.6838(14)
β, deg	100.807(14)	100.952(7)
Volume, Å^3	926.90(11)	917.01(17)
$Z(Z')$	4(1)	4(1)
Density (calcd.), g/cm^3	1.435	1.450

collected in the 7.34° to 68.12° θ range. The final refinement produced with anisotropic atomic displacement parameters for all atoms converged to R_1 = 0.0485, wR_2 = 0.1312. The unit cell parameters obtained for the single crystal are: a = 12.2879(9) Å, b = 4.8782(3) Å, c = 15.7423(12) Å, β =100.807(14)°, which indicates that the structure is monoclinic with the space group $P21/c$. The crystal packing of AHQ shows that the molecule is not planar (Fig. 4). The orientation of the azide group is defined by torsion angles C(5)–C(7)–C(12)–N(13) [80.75(19)°] and C(8)–C(7)–C(12)–N(13) [–96.42(18)°] obtained by X-ray crystallography (Table 3).

It is well known that the hydrogen bonds between the molecule and its environment play an important role in stabilization of the supramolecular structure formed with the neighboring molecules [29, 30]. The Fig. 5 and Table 2 show intra- and intermolecular hydrogen bonds present in the crystal structure of the AHQ. Weak intramolecular O–H···N hydrogen-bonding is present between the phenol donor and the adjacent pyridine N-atom acceptor [O11–N1 = 2.7580(17) Å and O11–H11···N1 = 115.1(16)°] (Fig. 5a). Moderate intermolecular O–H···N hydrogen bond is also present [O11–N11 = 2.8746(17) Å and O11–H11···N1 = 130.1(17)°]. The acceptor function of oxygen atom is employed by two weak intermolecular C–H···O hydrogen bonds, which parameters values are reported in Table 2. Because of the intramolecular hydrogen bonding, the phenol ring is twisted slightly, the torsion angle N(1)–C(6)–C(10)–O(11) is 1.9(2)°. In addition, all the H-bonds involving neighboring molecules are practically in the same rings plane (Fig. 5b).

The standard geometrical parameters were minimized at DFT (B3LYP) level with 6-311G(*d*,*p*) basis set, then re-optimized again at HF level using the same basis set [28] for better description. Initial geometry generated from X-ray refinement data and the optimized structures were confirmed to be minimum energy conformations. The energy and dipole

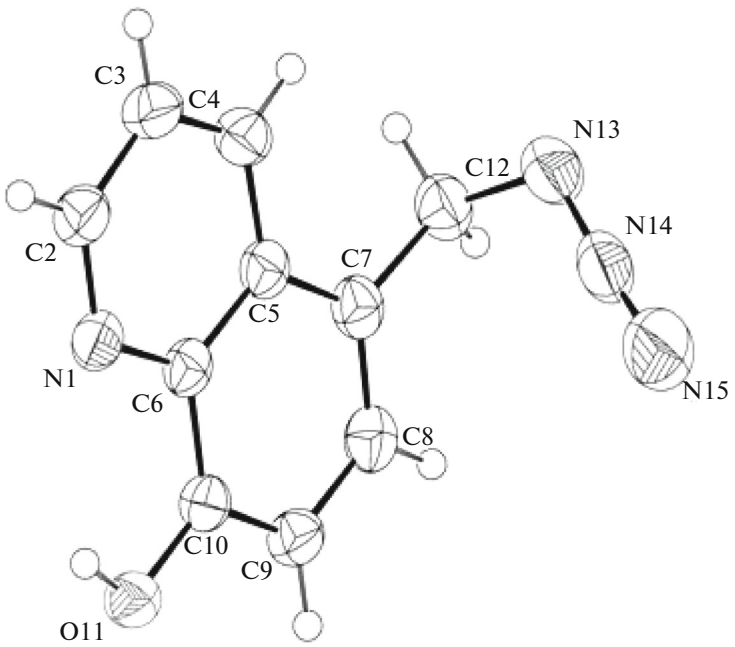

Fig. 3. ORTEP drawing of AHQ showing the atom numbering. Displacement ellipsoids are drawn at the 50% probability level. H atoms are represented as small circles.

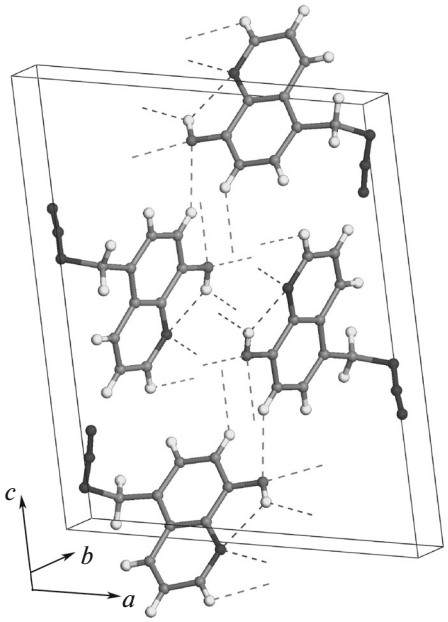

Fig. 4. Crystal packing the AHQ chains.

moments for DFT and HF methods are respectively −18501.70 eV and 2.5114 D, −18388.96 eV and 2.2864 D.

The molecular structure of AHQ by optimized DFT (B3LYP) is shown in Fig. 6. The geometry parameters available from experimental data (1), optimized by DFT (B3LYP) (2) and HF (3) of the molecule are presented in Table 3. The calculated and experimental structural parameters for each method were compared.

As seen from Table 3, most of the calculated bond lengths and the bond angles are in good agreement with experimental ones. The highest differences are observed for N(1)–C(6) bond with a value 0.012 Å for DFT method and N(14)–N(15) bond with the difference being 0.037 Å for HF method.

For the bond angles those differences occur at O(11)–C(10)–C(9) bond angle with the different value 4.64° for DFT method, and O(11)–C(10)–C(9) bond angle with a value 4.75° for HF method. When the X-ray structure of AHQ is compared to the optimized one, the most notable discrepancy is observed in the orientation of the azide moiety, which is defined by torsion angles C(5)–C(7)–C(12)–N(13) [80.75(19)°] and C(7)–C(12)–N(13)–N(14) [47.0(2)°] obtained by X-ray crystallography, these torsion angles have been calculated to be −66.5778°, −62.3307° for DFT and −65.2385°, −62.3058° for HF, respectively. This shows the larger deviation from the experimental values because the theoretical calculations have been performed for isolated molecule whereas the experimental data has been recorded in solid state and are related to molecular packing [31].

Figure 7 shows the patterns of the HOMO and LUMO of 5-azidomethyl-8-hydroxyquinoline molecule calculated at the B3LYP level. Generally this diagram shows the charge distribution around the different types of donors and acceptors bonds presented in the molecule in the ground and first excited states. HOMO as an electron donor represents the ability to donate an electron, while LUMO as an electron acceptor represent the ability to receive an electron

Table 2. Geometry of the intra- and intermolecular hydrogen bonds

D	H	A	D–H (Å)	H···A (Å)	D···A (Å)	D–H···A (deg)	Symmetry
O11	H11	N1	0.88(2)	2.27(2)	2.7580(17)	115.1(16)	1
O11	H11	N1	0.88(2)	2.23(2)	2.8746(17)	130.1(17)	2
C2	H2	O11	0.9300	2.55	3.0638(19)	115.0	3
C9	H9	O11	0.9300	2.57	3.3319(18)	139. 0	3

Symmetry codes: 1: x, y, z; 2: $1 - x, -y, -z$; 3: $1 - x, 1/2 + y, 1/2 - z$.

Table 3. Structural parameters of AHQ determined experimentally by X-ray diffraction (1) and calculated by the DFT/B3LYP/6-311G(*d*,*p*) (2) and HF/6-311G(*d*,*p*) (3) methods

Parameters	(1)	(2)	(3)	Parameters	(1)	(2)	(3)
Bond length (Å)				Torsion angles (deg)			
N(1)–C(2)	1.323(2)	1.3148	1.2905	C(6)–N(1)–C(2)–C(3)	–0.4(2)	0.3276	0.2157
N(1)–C(6)	1.368(2)	1.3564	1.3483	N(1)–C(2)–C(3)–C(4)	0.2(3)	–0.3281	–0.1238
C(2)–C(3)	1.411(2)	1.4119	1.4122	C(2)–C(3)–C(4)–C(5)	0.0(2)	–0.2358	–0.263
C(3)–C(4)	1.368(2)	1.3725	1.3562	C(3)–C(4)–C(5)–C(6)	0.0(2)	0.726	0.5221
C(4)–C(5)	1.422(2)	1.4181	1.4184	C(3)–C(4)–C(5)–C(7)	–179.68(14)	–179.2694	–179.2311
C(5)–C(6)	1.426(2)	1.4295	1.4042	C(2)–N(1)–C(6)–C(5)	0.4(2)	0.2335	0.084
C(5)–C(7)	1.430(2)	1.4306	1.4334	C(2)–N(1)–C(6)–C(10)	179.60(13)	–179.7015	–179.93
C(6)–C(10)	1.431(2)	1.4344	1.4338	C(4)–C(5)–C(6)–N(1)	–0.1(2)	–0.7516	–0.4466
C(7)–C(8)	1.375(2)	1.3763	1.3559	C(7)–C(5)–C(6)–N(1)	179.51(12)	179.244	179.3137
C(7)–C(12)	1.509(2)	1.509	1.5114	C(4)–C(5)–C(6)–C(10)	–179.36(12)	179.1829	179.5676
C(8)–C(9)	1.409(2)	1.4098	1.4155	C(7)–C(5)–C(6)–C(10)	0.3(2)	–0.8215	–0.672
C(9)–C(10)	1.370(2)	1.3774	1.3564	C(4)–C(5)–C(7)–C(8)	178.69(14)	–178.9396	–179.5629
C(10)–O(11)	1.3563(18)	1.3531	1.3385	C(6)–C(5)–C(7)–C(8)	–0.9(2)	1.0652	0.6932
C(12)–N(13)	1.502(2)	1.4936	1.4772	C(4)–C(5)–C(7)–C(12)	1.5(2)	1.6784	1.1591
N(13)–N(14)	1.234(2)	1.2309	1.2274	C(6)–C(5)–C(7)–C(12)	–178.15(13)	–178.3168	–178.5849
N(14)–N(15)	1.131(2)	1.1345	1.094	C(5)–C(7)–C(8)–C(9)	0.8(2)	–0.6271	–0.2842
Bond angle (deg)				C(12)–C(7)–C(8)–C(9)	178.02(14)	178.7626	179.002
C(2)–N(1)–C(6)	117.28(13)	118.0552	118.6007	C(7)–C(8)–C(9)–C(10)	0.1(2)	–0.0655	–0.1458
N(1)–C(2)–C(3)	123.78(15)	123.7195	123.5241	C(8)–C(9)–C(10)–O(11)	178.65(13)	–179.6956	–179.8307
C(4)–C(3)–C(2)	119.18(15)	118.8619	118.6443	C(8)–C(9)–C(10)–C(6)	–0.8(2)	0.3203	0.1699
C(3)–C(4)–C(5)	119.93(15)	119.7422	119.6045	N(1)–C(6)–C(10)–O(11)	1.9(2)	0.0783	0.2524
C(4)–C(5)–C(6)	116.15(14)	116.4268	116.4961	C(5)–C(6)–C(10)–O(11)	–178.84(13)	–179.8596	–179.7611
C(4)–C(5)–C(7)	124.17(14)	123.304	123.1178	N(1)–C(6)–C(10)–C(9)	–178.71(13)	–179.9365	–179.7482
C(6)–C(5)–C(7)	119.68(14)	120.2692	120.3857	C(5)–C(6)–C(10)–C(9)	0.6(2)	0.1255	0.2383
N(1)–C(6)–C(5)	123.68(14)	123.1894	123.1282	C(8)–C(7)–C(12)–N(13)	–96.42(18)	114.0507	115.4984
N(1)–C(6)–C(10)	117.03(13)	117.9498	117.7968	C(5)–C(7)–C(12)–N(13)	80.75(19)	–66.5778	–65.2385
C(5)–C(6)–C(10)	119.29(13)	118.8608	119.0749	C(7)–C(12)–N(13)–N(14)	47.0(2)	–62.3307	–62.3058
C(8)–C(7)–C(5)	118.51(14)	118.449	118.2338	C(12)–N(13)–N(14)–N(15)	–169(2)	–178.76649	–177.8718
C(8)–C(7)–C(12)	119.84(14)	120.1703	120.3364				
C(5)–C(7)–C(12)	121.60(14)	121.3778	121.4258				
C(7)–C(8)–C(9)	122.43(14)	122.0686	122.1105				
C(10)–C(9)–C(8)	120.10(14)	120.663	120.5675				
O(11)–C(10)–C(9)	118.72(13)	123.3691	123.4783				
O(11)–C(10)–C(6)	121.28(13)	116.9491	116.8978				
C(9)–C(10)–C(6)	119.99(14)	119.6818	119.6239				
N(13)–C(12)–C(7)	113.14(14)	114.6997	114.835				
N(14)–N(13)–C(12)	113.25(15)	115.5759	113.2348				
N(15)–N(14)–N(13)	174.8(2)	173.83049	175.6352				

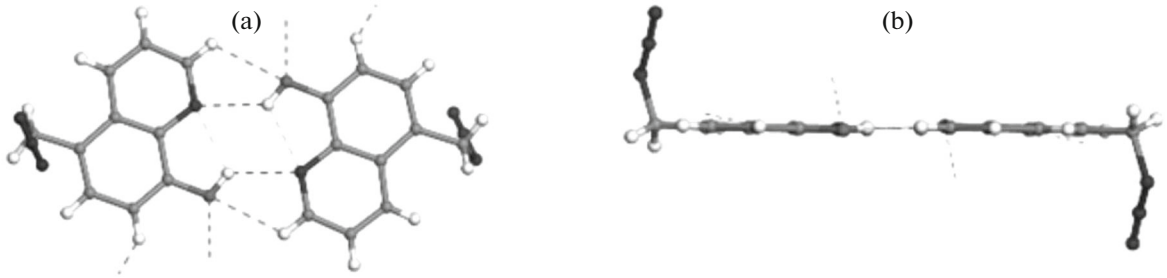

Fig. 5. View of H-bonding as dashed lines, H atoms not involved are omitted.

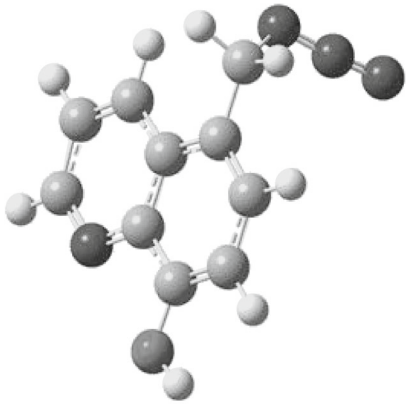

Fig. 6. Optimized structure of AHQ computed by the DFT/B3LYP/6-311G(*d*,*p*) method.

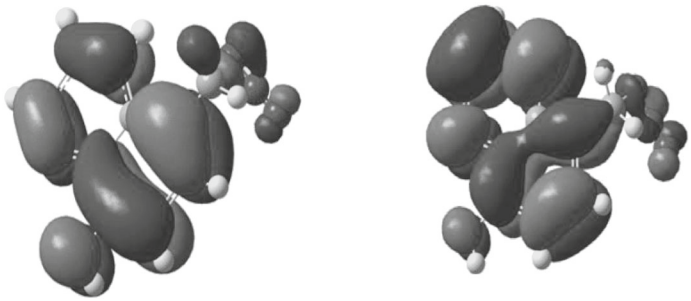

Fig. 7. Molecular orbital surfaces and energy levels for the HOMO, LUMO of the AHQ compound computed at DFT/B3LYP/6-311G (*d*,*p*) level.

[32–34]. The energy values of LUMO, HOMO and their energy gap reflect the chemical activity of the molecule. In our case, the calculated energy values of HOMO is –6.165424 eV and LUMO is –1.726656 eV in gaseous phase. The energy separation between the HOMO and LUMO is 4.438768 eV, this lower value of HOMO–LUMO energy gap is generally associated with a high chemical reactivity [35, 36], explains the eventual charge transfer interaction within the molecule, which is responsible for the bioactive properties of AHQ [37].

Supplementary Material

Crystallographic data for the structure of 5-azidomethyl-8-hydroxyquinoline have been deposited at the Cambridge Crystallographic Data Center (CCDC 1029534). This information may be obtained on the web: http//www.ccdc.cam.ac.uk/deposit.

CONCLUSION

In the present work, 5-azidomethyl-8-hydroxyquinoline was synthesized and its chemical structure

was confirmed using ^{1}H NMR, ^{13}C NMR and X-ray diffraction. The DSC analysis revealed no solid–solid transition for this product. The unit cell parameters obtained for the single crystal are: $a = 12.2879(9)$ Å, $b = 4.8782(3)$ Å, $c = 15.7423(12)$ Å, $\beta = 100.807(14)°$ which indicates that the structure is monoclinic, $P2_1/c$, with $Z = 4$ and $Z' = 1$.

The crystal structure is stabilized by intra and intermolecular O–H···N and C–H···O hydrogen bonds. This system of hydrogen bonds involves two neighboring molecules in the same plane. The geometric parameters of AHQ compound in ground state, calculated by density functional theory (B3LYP) and Hartree-Fock (HF) methods with the 6-311G(*d*,*p*) basis set, are in good agreement with the X-ray, except torsion angles which showed the deviation from the experimental, because of the geometry of the crystal structure is subject to intermolecular forces, such as van der Waals interactions and crystal packing forces, while only intramolecular interactions were considered for isolated molecule. The energy gap was found using HOMO and LUMO calculations, the less band gap indicates an eventual charge transfer within the molecule.

REFERENCES

1. M. di Vaira, C. Bazzicalupi, P. Orioli, L. Messori, B. Bruni, and P. Zatta, Inorg. Chem. **43**, 3795 (2004).
2. A. Mellah and D. Benachour, Hydrometallurgy. **81**, 100 (2006).
3. A. Albert and J. N. Phillips, Chem. Soc. **264**, 1294 (1956).
4. R. Kayyali, A. S. Pannala, H. Khodr, and R. C. Hider, Biochem Pharmacol. **55**, 1327 (1998).
5. I. Cacciatore, E. Fornasari, L. Baldassare, C. Cornacchia, S. Fulle, E. S. di Filippo, T. Pietrangelo, and F. Pinnen, Pharm. **6**, 54 (2013).
6. Y. Hamada, IEEE Trans. Electron Devices. **44**, 1208 (1997).
7. C. H. Chen and Shi Jianmin, J. Coord. Chem. Rev. **171**, 161 (1998).
8. D. H. Mathew and H. B. Schlegel, Chem. Mater. **13**, 2632 (2001).
9. V. A. Montes, R. Pohl, J. Shinar, and P. Anzenbacher, Jr., Chem. Eur. J. **12**, 4523 (2006).
10. G. N. Lipunovaab, E. V. Nosovaab, V. N. Charushinab, and O. N. Chupakhinab, Comm. Inorg. Chem. **34**, 142 (2014).
11. G. E. Collis, A. K. Burrell, K. D. John, and P. G. Plieger, Acta Crystallogr. C **59**, 0443 (2003).
12. C. H. Chen and J. M. Shi, Coord. Chem. Rev. **171**, 161 (1998).
13. A. Y. Shen, S. N. Wu, and C. T. Chiu, J. Pharm. Pharmacol. **51**, 543 (1999).
14. D. Mechlovich, T. Amit, S. A. Mandel, O. Bar-Am, K. Bloch, M. B. H. Vardi, and P. Youdim, J. Pharmacol. Exp. Ther. **333**, 874 (2010).
15. C. I. Nieto, M. A. Garcia, M. A. Farran, R. M. Claramunt, M. C. Torralba, M. R. Torres, I. Alkorta, and J. Elguero, J. Mol. Struct. **1008**, 88 (2012).
16. R. Desiderato, J. C. Jerry, and G. R. Freemant, Acta Crystallogr. B **27**, 2443 (1971).
17. D. E. Pearson, R. D. Wysong, and C. V. Breder, J. Org. Chem. **32**, 2358 (1967).
18. H. Gershon, M. W. McNeil, and A. T. Grefig, J. Org. Chem. **34**, 3268 (1969).
19. K. Hunger, *Industrial Dyes, Chemistry, Properties, Applications* (Wiley-VCH, Weinheim, 2003).
20. M. La Deda, A. Grisolla, I. Aiello, A. Crispini, M. Ghedini, S. Belviso, M. Amati, and F. Lelj, J. Chem. Soc., Dalton Trans. **16**, 2424 (2004).
21. A. Saylam, Z. Seferoglu, and N. Ertan, J. Mol. Liq. **195**, 267 (2014).
22. B. Himmi, B. Messnaoui, S. Kitane, A. Eddaif, A. Alaoui, A. Bouklouz, and M. Soufiaoui, Hydrometallurgy **93**, 39 (2008).
23. M. Labrador, M. A. Cuevas-Diarte, D. Mondieig, and Y. Haget, Thermochim. Acta **195**, 261 (1992).
24. H. M. Rietveld, J. A. Crystallog. **2**, 65 (1969).
25. G. Sheldrick, *SHELXS-97 Program for the Refinement of Crystal Structure* (Univ. Göttingen, Göttingen, Germany, 1997).
26. A. El Assyry, B. Benali, A. Boucetta, and B. Lakhrissi, J. Mater. Environ. Sci. **5**, 1860 (2014).
27. Y. Li, Y. Y. Liu, X. J. Chen, X. H. Xiong, and F. S. Li, PLoS ONE **9**, e91361 (2014).
28. M. J. Frisch et al., *Gaussian 03, Revision D.01 and D.02* (Gaussian Inc., Wallingford, CT, 2005).
29. A. Kadiri, B. Kabouchi, B. Benali, C. Cazeau-Dubroca, and G. Nouchi, Spectrochim. Acta, Part A **50**, 1 (1994).
30. C. Cazeau-Dubroca, Trends Phys. Chem. **2**, 233 (1991).
31. K. Aggarwal and J. M. Khurana, J. Mol. Struct. **1079**, 21 (2015).
32. C. Lee, W. Yang, and R. G. Parr, J. Phys. Rev. B **37**, 785 (1998).
33. Y. Ataly, D. Avci, and A. Basoglu, J. Struct. Chem. **19**, 239 (2008).
34. Y. Chen, J. Wu, S. Ma, S. Zhou, X. Meng, L. Jia, and Zhiquan Pan, J. Mol. Struct. **1089**, 1 (2015).
35. K. Fukui, Science **218**, 747 (1982).
36. S. Gunasekaran, R. A. Balaji, S. Kumeresan, G. Anand, and S. Srinivasan, Can. J. Anal. Sci. Spectrosc. **53**, 149 (2008).
37. D. Arul Dhas, I. Hubert Joe, S. D. D. Roy, and T. H. Freeda, Spectrochim. Acta, Part A **77**, 36 (2010).